



Monitoring magnesium degradation using microdialysis and fabric-based biosensors

[Natasha Su](#), [Malon Radha](#), [Wicaksono Dedy](#), [Corcoles Emma](#) and [Hermawan Hendra](#)

Citation: [SCIENCE CHINA Materials](#) ; doi: 10.1007/s40843-017-9069-3

View online: <http://engine.scichina.com/doi/10.1007/s40843-017-9069-3>

Published by the [Science China Press](#)

Articles you may be interested in

[In vivo electrochemical recording of continuous change of magnesium in medial vestibular nucleus following vertigo induced by ice water vestibular stimulation](#)

SCIENCE CHINA Chemistry **56**, 256 (2013);

[Biocompatibility of bio-Mg-Zn alloy within bone with heart, liver, kidney and spleen](#)

Chinese Science Bulletin **54**, 484 (2009);

[Cell-based biosensors: Towards the development of cellular monitoring](#)

Chinese Science Bulletin **47**, 1849 (2002);

[Applications of polymer single nanochannels in biosensors](#)

Chinese Science Bulletin **58**, 1473 (2013);

[ZnO nanostructures in enzyme biosensors](#)

SCIENCE CHINA Materials **58**, 60 (2015);

Monitoring magnesium degradation using microdialysis and fabric-based biosensors

Journal:	<i>SCIENCE CHINA Materials</i>
Manuscript ID	SCMs-2017-0086.R1
Manuscript Type:	Article
Date Submitted by the Author:	24-Jun-2017
Complete List of Authors:	Natasha, Su; Universiti Teknologi Malaysia Malon, Radha; Universiti Kebangsaan Malaysia Wicaksono, Dedy; Swiss German University Corcoles, Emma; Instituto de Microelectronica de Barcelona Hermawan, Hendra; Laval University, Materials Engineering
Keywords:	biodegradable metal, biosensor, fabric device, magnesium, microdialysis
Speciality:	biodegradable metal

SCHOLARONE™
Manuscripts

Monitoring magnesium degradation using microdialysis and fabric-based biosensors

M.S. Natasha^{a†}, R.S.P. Malon^{a,b†}, D.H.B. Wicaksono^{a,c}, E.P. Córcoles^{a,d}, H. Hermawan^{a,e*}

^aFaculty of Biosciences and Medical Engineering, Universiti Teknologi Malaysia, 81310 Johor Bahru, Malaysia

^bFaculty of Science and Technology, Universiti Kebangsaan Malaysia, 43600 Bangi, Selangor Darul Ehsan, Malaysia

^cDepartment of Biomedical Engineering, Faculty of Life Sciences and Technology, Swiss German University, Tangerang 15143, Indonesia

^dInstituto de Microelectrónica de Barcelona (IMB-CNM), CSIC, Campus UAB, 08193 Bellaterra, Spain

^eDepartment of Mining, Metallurgical and Materials Engineering & CHU de Québec Research Center, Quebec City, G1V 0A6, Canada

[†]Equal contribution

*Corresponding author (e-mail: hendra.hermawan@gmn.ulaval.ca)

ABSTRACT This paper describes the development of a monitoring system capable of detecting the concentration of magnesium ions (Mg^{2+}) released during the degradation of magnesium implants. The system consists of a microdialysis probe that samples fluid adjacent to the implant and a catalytic biosensor specific to Mg^{2+} ions. The biosensor was fabricated on a cotton fabric platform, in which a mixture of glycerol kinase and glycerol-3-phosphate oxidase enzymes were immobilized on the fabric device via a simple matrix entrapment technique of the cotton fibers. Pure magnesium was used as the implant material. Subsequently, the concentration of ions released from the degradation of the magnesium specimen in Ringer's solution was evaluated using cyclic voltammetry technique. The device demonstrated a pseudo-linear response from 0.005 mM to 0.1 mM with a slope of 67.48 $\mu A/mM$. Detectable interfering species were lesser than 1% indicating a high selectivity of the fabric device. Furthermore, the device requires only 3 μL of fluid sample to complete the measurement compared to spectroscopic method ($\pm 50 \mu L$), hence providing a higher temporal resolution and reduced sampling time. The system could potentially provide a real time assessment of the degradation behavior, an uncommon studied aspect in biodegradable metals research.

Keywords: biodegradable metal, biosensor, fabric device, magnesium, microdialysis

INTRODUCTION

The human body is considered as an aggressive environment for implanted metal alloys due to its highly oxygenated saline electrolyte [1]. Hence, for decades, it has been agreed that an ideal material for a metal implant must be corrosion-resistant. However, the paradigm has been shifted by the introduction of biodegradable metals as the model material for implants assisting the treatment of temporary clinical problems [2]. Magnesium, iron, zinc and their alloys are the three types of metals that have been studied as biodegradable metals, metals that degrade in physiological environment via corrosion. In this article, the term of corrosion is therefore interchangeable with degradation. Magnesium possesses interesting mechanical properties, where its Young's modulus and compressive strength are close to those of cortical bone [3, 4]. Magnesium-based biodegradable metals have received attention on almost every aspects of research including material development, *in vitro* degradation, *in vivo* animal studies, pre-clinical trials and commercialization since their first introduction in 2003 [5-9]. However, one aspect was

1
2
3 least considered, the measurement of its degradation kinetics continuously using a rapid
4 detection technique. This measurement will further enable the study of *in vivo* degradation of
5 magnesium or other biodegradable metal implants, thus allowing a better design of implants.
6
7
8

9
10 The most used techniques to assess the *in vivo* degradation of biodegradable metals include
11 implant retrieval analysis assisted by scanning electron microscope (SEM), X-ray diffraction
12 (XRD) and energy dispersive X-ray spectroscopy (EDS) [10]; non-invasive microtomography
13 (micro-CT) [11], [12]; X-ray radiography [13] and the least accessible synchrotron micro-CT
14 [14, 15]. These techniques are capable of revealing the degradation mechanism of the implant,
15 including the determination of degradation products and its composition; however no real time
16 data can be obtained especially on the degradation kinetics. Studies that assessed the continuous
17 degradation measurements are much more recent. Schumacher *et al.* [16] used microdialysis to
18 investigate the reaction interface between pure magnesium and tissue in isolated perfused bovine
19 udder model and examined its biocompatibility using prostaglandin E2 (PGE2) and tumor
20 necrosis factor alpha (TNF- α) concentrations, which served as indicators of inflammation.
21 Although their work has managed to penetrate the *ex vivo* behavior of the implant, the results
22 were not measured in real time because they still rely on the offline spectrophotometric
23 measurements. Another work by Ulrich *et al.* [17] utilized a micro-flow-capillary (μ FC) that was
24 online-coupled via a flow injection analyzing system (FIAS) to an inductively coupled plasma
25 mass spectrometer (ICP-MS) setup with electrochemical control to investigate the degradation
26 behavior of magnesium alloys. However, the generated hydrogen (H_2) gas bubbles were
27 suspected to prevent sufficient mixing in the circulating solution within the capillary, hence lack
28 of accuracy was reported in the results. A latest work by Zhao *et al.* [18] measured the real-time
29 concentration of magnesium ions, hydroxyl ions and hydrogen gas using sensory system
30 composed of in-house capillary pH and Mg^{2+} microsensors and a hydrogen gas sensor. The
31 sensor was able to map the hydrogen concentration in the vicinity of an implanted magnesium
32 alloy. The group continued their work by developing a transdermally electrochemical hydrogen
33 microsensor and tested it for measuring the biodegradation of various magnesium implants in
34 mouse. The sensor was able to easily detect hydrogen at the concentration as low as 30–400 μ M
35 permeating through the skin with a fast response time of 30 seconds. However, due to the
36
37
38
39
40
41
42
43
44
45
46
47
48
49
50
51
52
53
54
55
56
57
58
59
60

1
2
3 dependence to the skin permeability that the hydrogen can permeate through, this technique
4 might not be applicable to deep implants such as on the thigh bone [19, 20].
5
6

7
8 Chemical sensors such as ion selective electrodes (ISE) are capable of detecting fluid variables
9 such as pH and concentration of various ions (Mg^{2+} , K^+ , Ca^{2+} , etc.). Magnesium ion selective
10 electrodes (Mg-ISE) have been essentially used to determine intracellular free Mg^{2+} ions
11 concentration [21]. However, the development process is often complicated and it exhibits
12 limited selectivity since Ca^{2+} ions are a common interfering species [22]. Biosensors using
13 enzymes as the bio-recognition molecule are recognized for their high selectivity and specificity,
14 whilst electrochemical biosensors are the most popular choices for their sensitivity [23].
15 Nevertheless, both ISE and electrochemical biosensors consist of electrodes that are constituted
16 by metal, typically platinum, hence presenting biocompatibility issues. When the sensor is
17 implanted in tissue, it is recognized as a foreign body by the immune system, which triggers a
18 cascade immune response. Proteins and blood vessels form a capsule around the sensor
19 (biofouling), consequently compromising its sensing capabilities [24]. In order to overcome this
20 issue, microdialysis has been used over the last 30 years and coupled to a range of detection
21 techniques among which are biosensors. Microdialysis, a sampling technique first developed to
22 mimic a blood capillary, was used to sample neurochemicals from a rodent's brain [25]. Over the
23 years, microdialysis has been used for other tissues such as gastrointestinal [26] and
24 cardiovascular [27] as well as implanted subcutaneously or intravenously [27, 28]. Microdialysis
25 use has been reported for up to five days in patients allowing to sample ions and small molecules
26 without extracting blood cells or other large components due to the membrane small molecular
27 weight cut-off [29]. Microdialysis combined with biosensors presents a synergetic effect
28 allowing a real-time monitoring of degradation process. Microdialysis overcomes the
29 biocompatibility issues of biosensors, while biosensors increase the temporal resolution of the
30 sampling technique. A microdialysis probe can be inserted beneath the skin thus allowing a
31 degradation measurement of a deep implant. Therefore, in this study we aim to use microdialysis
32 coupled with magnesium biosensor to monitor the concentration of Mg^{2+} ions released from the
33 degradation of magnesium specimen in Ringer's solution. Success in developing this system *in*
34 *vitro* will allow a further exploration for future *in vivo* setting.
35
36
37
38
39
40
41
42
43
44
45
46
47
48
49
50
51
52
53
54
55
56
57
58
59
60

EXPERIMENTAL SECTION

Specimen preparation and fabrication of Mg²⁺ biosensor

Specimens (diameter = 3.2 mm, length = 10 mm) were prepared from pure magnesium rods (99.9% purity, Goodfellow, UK). They were polished using abrasive paper grit #1200, ultrasonically cleaned in ethanol at 30°C for 10 min, etched with 2% Nital solution to remove oxides, and finally rinsed with distilled water before drying in the desiccator for an hour. A fabric-based electrochemical device (FED) was used as described previously [30, 31] for the development of the Mg²⁺ biosensor. Cotton fabric provides an optimum and flexible platform for manual fabrication of electrodes. Furthermore, the hierarchical structure of the natural cellulose fibers allows a robust entrapment of enzymes within the fibers without requiring additional artificial membranes or chemicals for its immobilization [32]. Briefly, fabrication of the FED consists of a white plain cotton fabric (Jadi Batek Gallery, Malaysia) that was previously scoured using anhydrous sodium carbonate [30]. Conductive paste (Gwent Electronics Material, UK) was used to embed the electrodes onto the cotton fabric. Carbon graphite paste modified with Prussian blue (C-PB) was used for the working (WE) and counter (CE) electrodes, while silver/silver chloride (Ag/AgCl) paste was used for the reference electrode (RE). This procedure was followed by wax-patterning of the device in order to create a hydrophobic barrier for the area surrounding the sample placement/reaction zone. Then, two different enzymes were entrapped within the cellulose fibers of the FED. An amount of 20 mg/mL of each glycerol kinase (GK, 25-75 kU, *Cellulomonas* sp.) and glycerol-3-phosphate oxidase (GPOx, 70 kU, *Aerococcus viridians* sp.) enzymes (Sigma Aldrich, Malaysia) were dissolved in 0.1 M PBS. An amount of 3 μL of the enzyme mixture (4:1, GK:GPOx) was then drop-coated onto the reaction zone of the FED and left to dry at room temperature (~25 °C) for an hour. The Mg²⁺ biosensor functions based on the reaction of kinase enzyme which requires adenosine triphosphate (ATP) for the phosphorylation of the substrate and magnesium as a cofactor for the reaction to occur [33, 34]. The inset in Fig. 1 shows the mechanism of the reaction. Glycerol is phosphorylated by GK and the product of this reaction is then oxidized by GPOx which in turn produces hydrogen peroxide (H₂O₂). The H₂O₂ then reacts with the Prussian blue at the working electrode of the FED resulting in electrochemical signal that is proportional to the concentration of Mg²⁺, provided everything else remains constant.

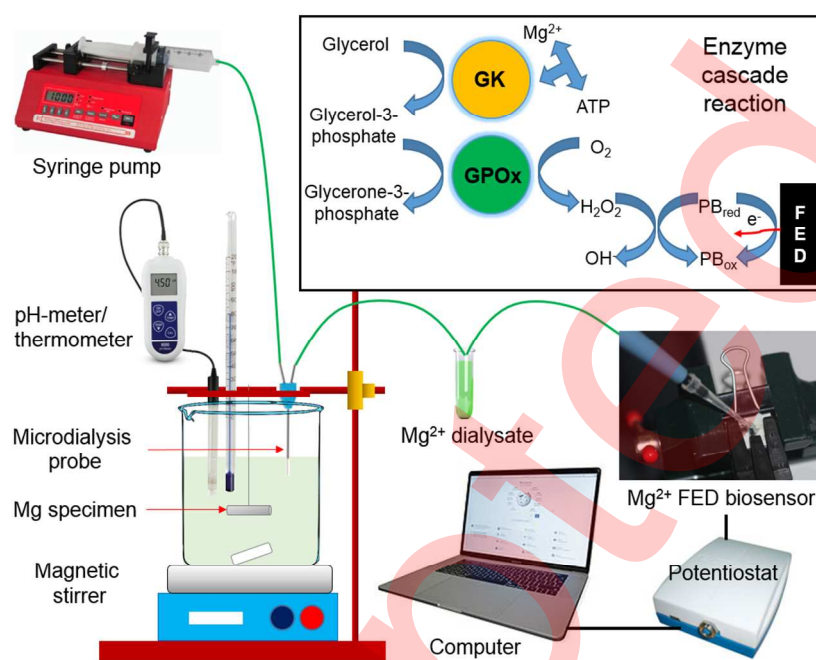


Figure 1 Schematic diagram of the experimental setup consisting of the microdialysis probe (sampling tool), FED (biosensor) and potentiostat/computer (converter chemical to electrical analysis). Dialysate is dropped at the sample placement (reaction zone) of the FED that was immobilized with the GK and GPOx enzymes to detect Mg^{2+} ions via enzymes cascade reaction (inset).

Immersion test and microdialysis sampling

The magnesium specimens were initial weighed (W_i), then immersed inside beakers (one specimen/beaker) containing a buffered Ringer's solution that consists of 118.4 mM sodium chloride (NaCl), 4.7 mM potassium chloride (KCl), 2.52 mM calcium chloride ($CaCl_2$), 1.18 mM monopotassium phosphate (KH_2PO_4) and 25.01 mM sodium bicarbonate ($NaHCO_3$) in 1 L of distilled water. All chemicals were of analytical reagents grade (Sigma Aldrich, Malaysia) unless stated otherwise. Three specimens were allowed to degrade in this solution for 1, 2 and 5 days, respectively. pH of the Ringer's solution was measured every 24 h for the period of 5 days. After the immersion test was completed, the corrosion product was removed from the specimens by immersing in chromate acid solution (200 g/L CrO_3 + 10 g/L $AgNO_3$) at ambient temperature for 5-10 min and rinsed thoroughly with distilled water before drying in the desiccator for 24 h [35]. This cleaning process was repeated until the final weight (W_f) of the specimens measured after

24 h became constant. The weight loss (mg) of the specimens ($W_i - W_f$) was then plotted against immersion time (hour). The result was used for making correlation between the degradation rate by weight loss and by Mg^{2+} concentration measured by the biosensor. The microdialysis (MD) probe (MAB 9.20.3 series, Microbiotech, Sweden) was immersed alongside the specimens during the immersion tests. The MD inlet was connected to a 1 mL syringe mounted on a NE-300 infusion syringe pump (New Era, Malaysia) and perfused with the Ringer's solution at a flow rate of 1.5 μ L/min for 90 min. At the outlet, the dialysate was collected in vials. Fig. 1 shows the experimental setup. Since the microdialysis probe recovers a percentage of the concentration of the bulk, the microdialysis recovery coefficient was determined by collecting a sample of the immersion solution using pipettes. Relative recovery (R) is a critical parameter that provides a percentage of the ratio between the concentration in the bulk (C_{bulk}) and the concentration in the dialysate (C_{dial}) [36], as per Equation 1:

$$R = \frac{C_{bulk}}{C_{dial}} \times 100\% \quad (1)$$

Electrochemical measurement of the device

A μ STAT400 portable potentiostat (Dropsens, Spain) was used for the electrochemical measurements. The electrodes were connected to the potentiostat using connector clips (Fig. 1). The electrochemical signals were measured and displayed using the manufacturer DropView software. Prior to the enzymes immobilization, characterization of the electrochemical behavior of C-PB was performed using cyclic voltammetry technique. For this purpose, 3 μ L of 0.1 M phosphate buffer solution (PBS) was placed at the sample placement region of the FED and cyclic voltammetry was performed at different scan rates (10, 25 and 50 mV/s). Next, the optimum detection potential of Mg^{2+} FED was investigated for the reliable detection of H_2O_2 (the product of the enzyme-catalyzed reaction) at the C-PB/GK/GPOx electrodes [31]. Since the substrate of the enzyme-catalyzed reaction is glycerol and not Mg^{2+} ion, the amount of glycerol required for the biosensor was investigated. Glycerol standards (0.05, 0.1, 0.2, 0.5, 1 and 3 mM) were prepared in a mixture of 3 mM magnesium chloride ($MgCl_2$), 3 mM ATP and 0.1 M PBS which are similar to those of the work of Ghica *et al.* [34]. An amount of 3 μ L of each glycerol standard was dropped at the sample placement region of the FED and cyclic voltammetry was performed at working potential range from -0.5 to +0.5 V at a potential scan rate of 10 mV/s. Cyclic voltammetry (CV) was used for the calibration of Mg^{2+} -FED biosensor with the Mg^{2+}

standards prepared using solution of MgCl_2 at a concentration range between 5 μM and 1 mM in 500 μM glycerol, 3 mM ATP and 0.1 M PBS at a potential scan rate of 10 mV/s. All the standards and buffer solutions were kept at 4°C when not in use. Fresh solutions were prepared weekly to retain freshness. For interference testing, common metabolites and biomolecules present in physiological fluids such as 0.2 mM of D-(+)-glucose ($\geq 99.5\%$), L-ascorbic acid (vitamin C) and urea ($\geq 99.5\%$) were added into 0.2 mM MgCl_2 standards (1:1 ratio of interferences to MgCl_2). The CV scans were then conducted at a potential scan rate of 10 mV/s within a working potential range from -0.5 to +0.5 V for all the interference solutions.

RESULTS AND DISCUSSION

Fig. 2a shows the variation of weight loss and pH of the Ringer's solution over the immersion time. Overall, the weight loss increases with the longer immersion time at 1.79 $\text{mg}/\text{cm}^2/\text{day}$. Similar increase is observed for the pH of the Ringer's solution over the immersion time. The oxidation of magnesium metal to Mg^{2+} ions on the anode is balanced by the reduction of water to form hydrogen gas and OH^- on the cathode. The weight loss over immersion time can be related to the general corrosion, a phenomenon previously reported by Wang *et al.* [37]. The higher increment of weight loss and pH on the period of day 1 to day 2 compared to the period of day 2 to day 5 could be related to the formation of adherent corrosion products (e.g. magnesium hydroxide and phosphates) on the specimen's surface that slows down corrosion process temporarily [38]. However, other factors beside the chemical reaction that contribute to the weight loss of magnesium during degradation were not considered in this study, such as the deposition of degradation products (MgCO_3 , CaCO_3 , NaCl) which increases the final weight, and the dissociation of broken piece of magnesium which reduces the final weight [39].

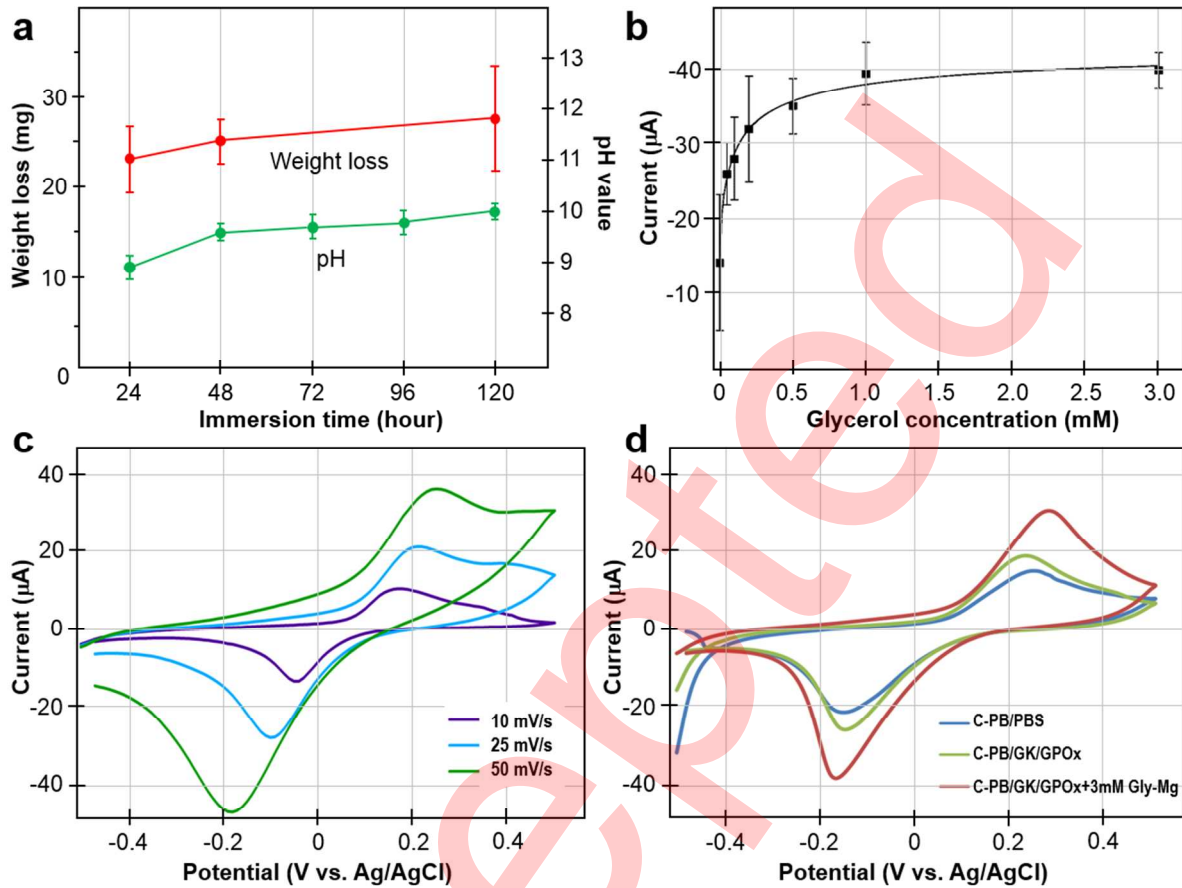
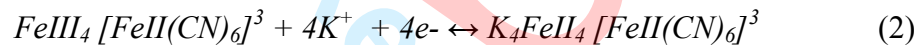


Figure 2 (a) Weight loss of magnesium specimens and pH of Ringer's solution from day 1 to 5; (b) calibration of Mg^{2+} -FED for glycerol samples (0.5 mM of glycerol provides the highest response before the saturation of the enzyme); (c) CV scan rate dependence on FED before immobilization was performed (measurements were taken at 10 mV/s, 25 mV/s and 50 mV/s scan rates); (d) CV curves of the C-PB electrodes at a range between -0.4 and +0.4 V in 0.1 M of PBS after modification with the GK and GPOx enzymes (C-PB/ GK/GPOx) and with 3 mM of glycerol/magnesium.

The enzyme-catalyzed reaction occurring on the C-PB/GK/GPOx electrodes is first due to the phosphorylation of glycerol. As mentioned in the method, Mg^{2+} ions are required as they act as cofactor for the reaction catalyzed by the kinase enzyme. When glycerol is kept constant, the current produced by the increase of the cofactor can be detected. Hence, the amount of glycerol required for the biosensor was investigated using different concentrations (0.05 - 3 mM) of glycerol standards in PBS solution with constant amounts of MgCl_2 and ATP. The CVs of the C-PB/GK/GPOx were performed using these glycerol standard solutions. The calibration curve for

glycerol was obtained from the cathodic current of the CV at potential of -0.2 V vs. Ag/AgCl. Fig. 2b shows the calibration curve of the sensor with glycerol standard solutions. The curve plateaus following the addition of 1 mM of glycerol indicating the saturation of the GK enzyme. The optimal response was chosen as that before saturation occurs, since it allowed the response to increase with an increase of Mg^{2+} ions concentration. Hence, the concentration of 0.5 mM of glycerol was selected to prepare the Mg^{2+} samples.

The 3 μ L of 0.1 M PBS were placed on the reaction zone and the CVs within the potential limits of -0.5 and +0.5 V at different potential scan rates (10, 25, 50 mV/s) were performed to characterize the electrochemical performance of the C-PB electrodes on the FED. Fig. 2c shows the CV characteristic indicating a diffusion controlled electron-transfer process similar to conventional electrochemical cells [31]. The anodic and cathodic peaks correspond to the following redox reaction (Equation 2):



In order to optimize the detection potential of the Mg^{2+} -FED biosensor for H_2O_2 detection, the C-PB/GK/GPOx electrodes were characterized using CV at a range between -0.4 and +0.4 V in 0.1 M of PBS (lack of H_2O_2). Results showed the characteristic redox peaks of PB, however, the peak current of C-PB/GK/GPOx was larger than the C-PB only, due to the increase in efficiency of the C-PB electrodes after modification with the GK and GPOx enzymes (Fig. 2d). An even larger peak current was observed when 3 mM of glycerol/magnesium was used compared with PBS only. The applied potential in the CV region between -0.2 and +0.2 V (H_2O_2 in C-PB electrodes region) was further investigated and the signal-to-background (S/B) ratios of each potential showed the highest S/B ratio at -0.2 V (data not shown). This low detection potential reduces the signal from common electrochemical interfering substance present in real samples.

Since the activity of enzymatic reaction is enhanced in the presence of Mg^{2+} ions, an increment in the concentration of Mg^{2+} provides a proportional increase in signal. After determining the optimal concentration of glycerol, CVs of the C-PB/GK/GPOx were obtained at different concentrations of Mg^{2+} standards solution (0 - 1 mM) as shown in Fig. 3a. The calibration curve (Fig. 3b) was obtained from the cathodic currents of the CV at a potential of -0.2 V vs Ag/AgCl.

The curve was fitted using a non-linear regression using the Hill's equation (Equation 3), which generates a sigmoid fit:

$$I = \frac{I_{max}}{1 + \left[\frac{K_M}{[S]}\right]^n} \quad (3)$$

Where, I is the current signal obtained, I_{max} is the maximum current signal, n is the Hill coefficient, $[S]$ is the concentration of substrate and K_M is the Michaelis-Menten constant, which is the $[S]$ value at $I_{max}/2$.

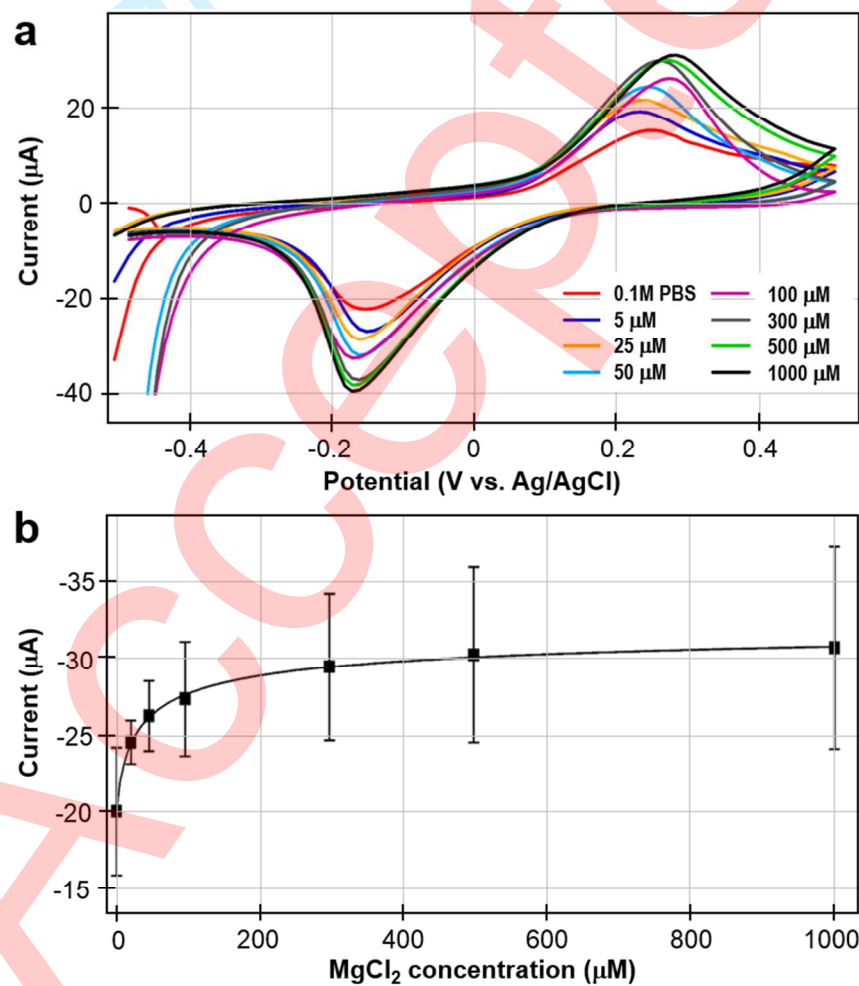


Figure 3 Calibration of Mg²⁺-FED for Mg²⁺ samples: (a) CV of different concentration of MgCl₂ to determine the sensitivity of FED biosensor, (b) non-linear regression of MgCl₂ fitted by the Hill's equation.

1
2
3 The Hill's equation coefficients of the Mg^{2+} biosensor coefficients were then calculated. I_{max} , the
4 current at what the signal plateaus, was $-32.81 \pm 0.38 \mu A$. The plateau response is a sign of the
5 saturation of the enzymes, the biorecognition molecules of the biosensor. Hence, high
6 concentration samples required to be diluted prior to the determination. The K_M of the enzymatic
7 mix used in this biosensor was $7.90 \pm 0.12 \text{ mM}$, which is the substrate concentration
8 corresponding to half of the maximum signal and n was the Hill coefficient, 0.48 ± 4.25 , which
9 denotes a cooperative binding. The calibration plot shows a pseudo-linear response from 0.005
10 mM until approximately 0.1 mM ($r^2 = 0.756$). From the slope of the linear calibration the
11 sensitivity of the sensor was calculated ($0.0679 \mu A/\text{mM}$). The limit of detection ($LOD = 10.162$
12 μM) and limit of quantification ($LOQ = 33.872$) of the device was calculated from standard
13 deviation (s) of the blank as the concentrations that produced the signal at 3s and 10s,
14 respectively for three separate devices. The repeatability of the device was calculated using the
15 same Mg^{2+} -FED three times for each Mg^{2+} concentration and the obtained relative standard
16 deviation (% RSD) was 5.71% for $25 \mu M$ of Mg^{2+} , while the reproducibility was measured using
17 three different devices for $50 \mu M$ and $1000 \mu M$ of Mg^{2+} , concentrations and the attained %RSD
18 was 8.64% and 21.4%, respectively.
19
20
21
22
23
24
25
26
27
28
29
30
31
32

33 Unlike the Mg^{2+} ion selective electrode, other bivalent metals such as Ca^{2+} or heavy metals does
34 not affect the FED response due to the specificity of the enzyme to the substrate, in this case
35 glycerol. Kinase enzyme uses Mg^{2+} ions as a cofactor, but other bivalent heavy metals do not
36 affect the kinetics of the reaction. On the other hand, although enzymes are specific
37 biorecognition molecules, other organic and electroactive substrates could sometimes produce an
38 electrochemical response. This could perturb the signal and cause misleading results. Therefore,
39 interferences testing were conducted to test the reliability of the sensor towards foreign
40 compounds. Ascorbic acids, glucose and urea are among the compounds that could interfere with
41 the chemical signal of the biosensor. The relative response with ascorbic acid was 1.26 %, then
42 1.18% with glucose and 1.13% with urea. Since the FED biosensor showed a rate of interference
43 of $\sim 1\%$ when exposed to a $200 \mu M$ of other chemicals, it was demonstrated that the sensor
44 presented a $\sim 99\%$ of selectivity.
45
46
47
48
49
50
51
52
53
54
55
56
57
58
59
60

Bulk and dialysate were tested on the FED to obtain current signals for each respective sample of different immersion days. Fig. 4a shows the bar graph of current signals for replications of bulk samples using three different FED sensors. The average current ($n=3$) for bulk samples on day 5 is $-50.33 \pm 2.46 \mu\text{A}$, whereas on day 1 is $-23.73 \pm 0.93 \mu\text{A}$. The increment of current signals is about two times higher within four days. This occurs due to the longer immersion of the magnesium sample in Ringers' solution, resulting in more Mg^{2+} ions being released. Subsequently, when a highly concentrated Mg^{2+} ions bulk solution was placed on the working region of FED, the catalyzed enzyme-substrate will produce more H_2O_2 . This compound (i.e. H_2O_2) is translated into electrical current signal proportional to the concentration of Mg^{2+} ions. The same phenomenon occurs for dialysate samples. However, the current produced for dialysate sample on day 5, which was supposed to be the highest current, was only $-31.18 \pm 0.66 \mu\text{A}$ (as seen in Fig. 4a). Increment has been linear for pure magnesium specimen without any sign of plateau after 5 days; hence we presumed longer times are required in order to observe the overall kinetics of the corrosion.

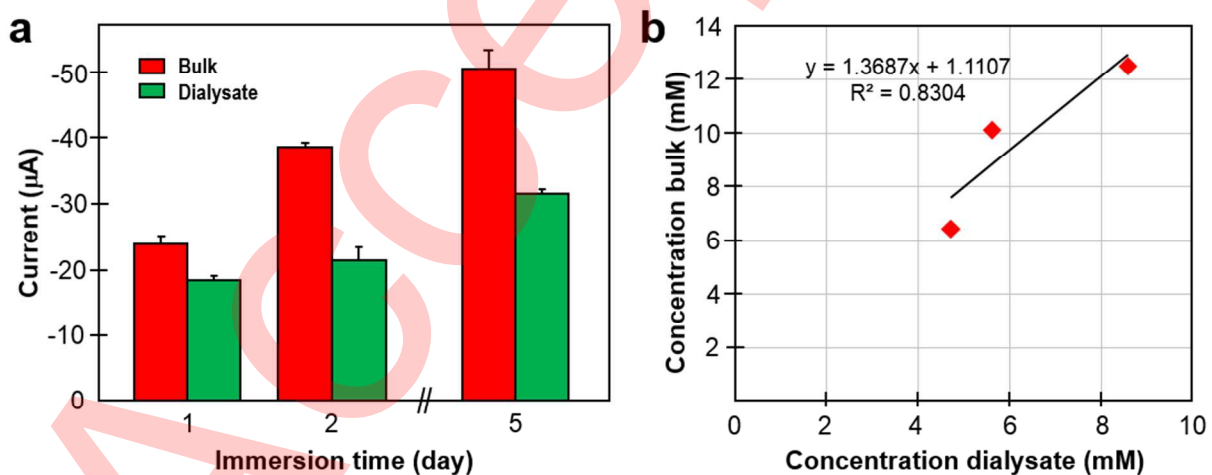


Figure 4 Measurement of: (a) current signal for bulk and dialysate samples up to 5 days immersion time; and (b) their linear correlation.

Clearly as shown in Fig. 4a, the current value of dialysate is lower compared to that of bulk samples. The linear regression correlation factor is 0.8304; while the chi-test's p-value is 0.1504, indicating a poor correlation between the two lines (Fig. 4b). However, this test was only done to find out the recovery of the probe and then be able to extrapolate them to an actual value of

1
2
3 **magnesium in the bulk.** Based on calibration, the Mg^{2+} concentrations in bulk/dialysate samples
4 for day 1, day 2 and day 5 are: 6.52/4.73, 10.17/5.61 and 12.56/8.60 mM, respectively. This
5 suggests that there are losses in the microdialysis membrane and that the total equilibrium cannot
6 be established with constant perfusion into microdialysis probe. From these results, we
7 calculated the recovery of samples (equation 1); are 72.56% in day 1, 55.17% in day 2 and
8 68.42% in day 5. The range of concentration losses **is between 55% and 73%**, where it could be
9 concluded that the recovery is very high. The rate at which these analytes were exchanged across
10 the semipermeable active membrane is expressed as the analyte extraction efficiency. This
11 calibration factor (recovery) shows that the efficiency of concentration gained in this study was
12 due to the low perfusion flow rate (i.e. 1.5 $\mu\text{L}/\text{min}$) that has been applied.
13
14
15
16
17
18
19
20
21
22

23 Finally, we analyze the correlation between degradation rate calculated from the weight loss and
24 from the Mg^{2+} concentration measured by the biosensor. The overall degradation rate calculated
25 from the weight loss at 5 days immersion time is 1.79 $\text{mg}/\text{cm}^2/\text{day}$. Using a simple stoichiometry
26 correlation of $\text{Mg} + 2\text{H}_2\text{O} \rightarrow \text{Mg}^{2+} + 2\text{OH}^- + \text{H}_2$, the corrosion rate calculated from the measured
27 concentration of Mg^{2+} in bulk on day 5 (12.56 mM) is 1.56 $\text{mg}/\text{cm}^2/\text{day}$. This tells a good
28 measurement has been obtained by the biosensor for the period of immersion test conducted in
29 this work. **Further improvement to the accuracy of the system can be done by carefully analyzing**
30 **other factors than chemical reaction that contribute to the weight loss of magnesium during**
31 **degradation (deposition of degradation products and dissociation of broken piece of magnesium),**
32 **verifying each calculated Mg^{2+} concentration using ICP-MS as well as setting-up an optimum**
33 **perfusion rate.**
34
35
36
37
38
39
40
41
42
43

44 CONCLUSIONS

45 A magnesium implant degradation monitoring system consisting of microdialysis sampling and
46 electrochemical detection with a fabric-based enzymatic biosensor has been successfully
47 developed and validated. The system measures Mg^{2+} samples at a small sample volume and more
48 frequent period, and thus reduces sampling time while increasing the temporal resolution. The
49 correlation was observed between the Mg^{2+} concentration in both the dialysate and the bulk. The
50 sensitivity of the biosensor is 67.48 $\mu\text{A}/\text{mM}$ with ~1% chance of interference and thus allows a
51 lower level Mg^{2+} detection. Although further studies are required in order to optimize the
52
53
54
55
56
57
58
59
60

1
2
3 combination between the biosensor and the microdialysis outlet, the system has shown the
4 capability to detect rapidly the dialysate Mg^{2+} levels electrochemically and could be suitable for
5 the monitoring *in vivo* degradation of Mg implants in real time.
6
7
8
9

10 References

- 11 1. Hansen DC. Metal corrosion in the human body: The ultimate bio-corrosion scenario.
12 Electrochem Soc Interface, 2008, 17: 31-34.
- 13 2. Nasution AK, Hermawan H. Degradable biomaterials for temporary medical implants. Adv
14 Struct Mater, 2016, 58: 127-160. http://dx.doi.org/10.1007/978-3-319-14845-8_6
- 15 3. Krause A, Von der Höh N, Bormann D, *et al.* Degradation behaviour and mechanical
16 properties of magnesium implants in rabbit tibiae. J Mater Sci, 2010, 45: 624-632.
17 <http://dx.doi.org/10.1007/s10853-009-3936-3>
- 18 4. Li K, Wang B, Chai J, *et al.* Electrochemical behaviour and cytocompatibility of nano-
19 fluoridated apatite coating on biodegradable magnesium alloy by simple chemical
20 conversion. Sci China Technol Sc, 2013, 56: 80-83. <http://dx.doi.org/10.1007/s11431-012-5018-z>
- 21 5. Heublein B, Rohde R, Kaese V, *et al.* Biocorrosion of magnesium alloys: A new principle
22 in cardiovascular implant technology? Heart, 2003, 89: 651-656.
23 <http://dx.doi.org/10.1136/heart.89.6.651>
- 24 6. Staiger MP, Pietak AM, Huadmai J, *et al.* Magnesium and its alloys as orthopedic
25 biomaterials: A review. Biomaterials, 2006, 27: 1728-1734.
26 <http://dx.doi.org/10.1016/j.biomaterials.2005.10.003>
- 27 7. Witte F, Hort N, Vogt C, *et al.* Degradable biomaterials based on magnesium corrosion.
28 Curr Opin Solid State Mater Sci, 2009, 12: 63-72.
29 <http://dx.doi.org/10.1016/j.cossms.2009.04.001>
- 30 8. Kirkland NT. Magnesium biomaterials: Past, present and future. Corr Eng Sci Technol,
31 2012, 47: 322-328. <http://dx.doi.org/10.1179/1743278212Y.0000000034>
- 32 9. Lee J, Han H, Han K, *et al.* Long-term clinical study and multiscale analysis of *in vivo*
33 biodegradation mechanism of Mg alloy. Proc Natl Acad Sci U S A, 2016, 113: 716-721.
34 <http://dx.doi.org/10.1073/pnas.1518238113>
- 35
36
37
38
39
40
41
42
43
44
45
46
47
48
49
50
51
52
53
54
55
56
57
58
59
60

10. Witte F, Kaese V, Haferkamp H, *et al.* In vivo corrosion of four magnesium alloys and the associated bone response. *Biomaterials*, 2005, 26: 3557-3563. <http://dx.doi.org/10.1016/j.biomaterials.2004.09.049>
11. Yang JX, Cui FZ, Lee I-S, *et al.* In vivo biocompatibility and degradation behavior of Mg alloy coated by calcium phosphate in a rabbit model. *J Biomater Appl*, 2012, 27: 153-164. <http://dx.doi.org/10.1177/0885328211398161>
12. Huehnerschulte TA, Reifenrath J, von Rechenberg B, *et al.* In vivo assessment of the host reactions to the biodegradation of the two novel magnesium alloys ZEK100 and AX30 in an animal model. *Biomed Eng Online*, 2012, 11: 14. <http://dx.doi.org/10.1186/1475-925X-11-14>
13. Ulum MF, Nasution AK, Yusop AH, *et al.* Evidences of in vivo bioactivity of Fe-bioceramic composites for temporary bone implants. *J Biomed Mater Res B*, 2015, 103: 1354-1365. <http://dx.doi.org/10.1002/jbm.b.33315>
14. Witte F, Fischer J, Nellesen J, *et al.* In vitro and in vivo corrosion measurements of magnesium alloys. *Biomaterials*, 2006, 27: 1013-1018. <http://dx.doi.org/10.1016/j.biomaterials.2005.07.037>
15. Witte F, Fischer J, Nellesen J, *et al.* In vivo corrosion and corrosion protection of magnesium alloy LAE442. *Acta Biomater*, 2010, 6: 1792-1799. <http://dx.doi.org/10.1016/j.actbio.2009.10.012>
16. Schumacher S, Stahl J, Baumer W, *et al.* Ex vivo examination of the biocompatibility of biodegradable magnesium via microdialysis in the isolated perfused bovine udder model. *Int J Artif Organs*, 2011, 34: 34-43. <http://dx.doi.org/10.5301/IJAO.2011.6332>
17. Ulrich A, Ott N, Tournier-Fillon A, *et al.* Investigation of corrosion behavior of biodegradable magnesium alloys using an online-micro-flow capillary flow injection inductively coupled plasma mass spectrometry setup with electrochemical control. *Spectrochim Acta B*, 2011, 66: 536-545. <http://dx.doi.org/10.1016/j.sab.2011.04.009>
18. Zhao D, Wang T, Guo X, *et al.* Monitoring biodegradation of magnesium implants with sensors. *JOM*, 2016, 68: 1204-1208. <http://dx.doi.org/10.1007/s11837-015-1775-z>
19. Zhao D, Wang T, Kuhlmann J, *et al.* In vivo monitoring the biodegradation of magnesium alloys with an electrochemical H₂ sensor. *Acta Biomater*, 2016, 36: 361-368. <http://dx.doi.org/10.1016/j.actbio.2016.03.039>

- 1
2
3
4
5
6
7
8
9
10
11
12
13
14
15
16
17
18
19
20
21
22
23
24
25
26
27
28
29
30
31
32
33
34
35
36
37
38
39
40
41
42
43
44
45
46
47
48
49
50
51
52
53
54
55
56
57
58
59
60
20. Zhao D, Wang T, Nahan K, *et al.* In vivo characterization of magnesium alloy biodegradation using electrochemical H₂ monitoring, ICP-MS, and XPS. *Acta Biomater*, 2017, 50: 556-565. <http://dx.doi.org/10.1016/j.actbio.2017.01.024>
 21. Altura B, Shirey T, Young C, *et al.* Characterization of a new ion selective electrode for ionized magnesium in whole blood, plasma, serum, and aqueous samples. *Scand J Clin Lab Invest Suppl*, 1994, 217: 21-36. <http://dx.doi.org/10.3109/00365519409095208>
 22. Günzel D, Schlue W-R. Determination of [Mg²⁺]_i – an update on the use of Mg²⁺-selective electrodes. *Biometals*, 2002, 15: 237-249. <http://dx.doi.org/10.1023/A:1016074714951>
 23. Gáspár S, Wang X, Suzuki H, *et al.* Amperometric biosensor-based flow-through microdetector for microdialysis applications. *Analyt Chim Acta*, 2004, 525: 75-82. <http://dx.doi.org/10.1016/j.aca.2004.07.041>
 24. Frost M, Meyerhoff ME. In vivo chemical sensors: tackling biocompatibility. *Analyt Chem*, 2006, 78: 7370-7377. <http://dx.doi.org/10.1021/ac069475k>
 25. Ungerstedt U, Pycock C. Functional correlates of dopamine neurotransmission. *Bulletin der Schweizerischen Akademie der Medizinischen Wissenschaften*, 1974, 30: 44.
 26. Córcoles EP, Deeba S, Hanna GB, *et al.* Use of online rapid sampling microdialysis electrochemical biosensor for bowel anastomosis monitoring in swine model. *Analyt Meth*, 2011, 3: 2010-2016. <http://dx.doi.org/10.1039/C1AY05306J>
 27. Abrahamsson P, Åberg AM, Johansson G, *et al.* Detection of myocardial ischaemia using surface microdialysis on the beating heart. *Clin Physiol Funct Imaging*, 2011, 31: 175-181. <http://dx.doi.org/10.1111/j.1475-097X.2010.00995.x>
 28. Mortensen SP, Thaning P, Nyberg M, *et al.* Local release of ATP into the arterial inflow and venous drainage of human skeletal muscle: Insight from ATP determination with the intravascular microdialysis technique. *J Physiol*, 2011, 589: 1847-1857. <http://dx.doi.org/10.1113/jphysiol.2010.203034>
 29. Feuerstein D, Manning A, Hashemi P, *et al.* Dynamic metabolic response to multiple spreading depolarizations in patients with acute brain injury: An online microdialysis study. *J Cereb Blood Flow Metab*, 2010, 30: 1343-1355. <http://dx.doi.org/10.1038/jcbfm.2010.17>

- 1
2
3
4
5
6
7
8
9
10
11
12
13
14
15
16
17
18
19
20
21
22
23
24
25
26
27
28
29
30
31
32
33
34
35
36
37
38
39
40
41
42
43
44
45
46
47
48
49
50
51
52
53
54
55
56
57
58
59
60
30. Nilghaz A, Wicaksono DHB, Gustiono D, *et al.* Flexible microfluidic cloth-based analytical devices using a low-cost wax patterning technique. *Lab Chip*, 2012, 12: 209-218. <http://dx.doi.org/10.1039/C1LC20764D>
 31. Malon RSP, Chua KY, Wicaksono DHB, *et al.* Cotton fabric-based electrochemical device for lactate measurement in saliva. *Analyst*, 2014, 139: 3009-3016. <http://dx.doi.org/10.1039/C4AN00201F>
 32. Bagherbaigi S, Corcoles EP, Wicaksono DHB. Cotton fabric as an immobilization matrix for low-cost and quick colorimetric enzyme-linked immunosorbent assay (ELISA). *Analyt Meth*, 2014, 6: 7175-7180. <http://dx.doi.org/10.1039/C4AY01071J>
 33. Compagnone D, Esti M, Messia MC, *et al.* Development of a biosensor for monitoring of glycerol during alcoholic fermentation. *Biosens Bioelectron*, 1998, 13: 875-880. [http://dx.doi.org/10.1016/S0956-5663\(98\)00055-4](http://dx.doi.org/10.1016/S0956-5663(98)00055-4)
 34. Emilia Ghica M, Brett CM. Development and applications of a bienzymatic amperometric glycerol biosensor based on a poly (neutral red) modified carbon film electrode. *Analyt Lett*, 2006, 39: 1527-1542. <http://dx.doi.org/10.1080/00032710600713198>
 35. Zhao M-C, Liu M, Song G, *et al.* Influence of the β -phase morphology on the corrosion of the Mg alloy AZ91. *Corr Sci*, 2008, 50: 1939-1953. <http://dx.doi.org/10.1016/j.corsci.2008.04.010>
 36. Plock N, Kloft C. Microdialysis—theoretical background and recent implementation in applied life-sciences. *Eur J Pharm Sci*, 2005, 25: 1-24. <http://dx.doi.org/10.1016/j.ejps.2005.01.017>
 37. Wang Y, Wei M, Gao J, *et al.* Corrosion process of pure magnesium in simulated body fluid. *Mater Lett*, 2008, 62: 2181-2184. <http://dx.doi.org/10.1016/j.matlet.2007.11.045>
 38. Ghoneim A, Fekry A, Ameer M. Electrochemical behavior of magnesium alloys as biodegradable materials in Hanks' solution. *Electrochim Acta*, 2010, 55: 6028-6035. <http://dx.doi.org/10.1016/j.electacta.2010.05.062>
 39. Tian Q, Deo M, Rivera-Castaneda L, Liu H. Cytocompatibility of magnesium alloys with human urothelial cells: A comparison of three culture methodologies. *ACS Biomater Sci Eng*, 2016, 2: 1559-1571. <http://dx.doi.org/10.1021/acsbiomaterials.6b00325>

Acknowledgements: This work was supported by the Malaysian Ministry of Education and the Natural Sciences and Engineering Research Council of Canada (NSERC).

Author contributions: All authors contributed to the preparation and discussion of the manuscript. The final version of the manuscript was approved by all authors.

Conflict of interest: The authors declare that they have no conflict of interest.



Emma Corcoles received her PhD degree in bioengineering from Imperial College London in 2009. She is now with the Instituto de Microelectrónica de Barcelona, Spain. Her research interests include electrochemical catalytic biosensors, immunosensors and other analytical techniques fabricated using different technologies and on different platforms and materials.



Dedy Wicaksono received his PhD degree in microelectronics from Delft University of Technology in 2008. He is now lecturer at the Swiss German University, Tangerang, Indonesia. His specialties include sensor and transducer design, physical modelling by analytical and numerical methods, characterization setup design and implementation, and device material process and characterization.



Hendra Hermawan received his PhD degree in materials engineering from Laval University in 2009. After spending some academic years in Asia, he returned to Laval University in 2014 as assistant professor and also researcher at CHU de Québec Research Center, Québec, Canada. His research interests include biomaterials, biodegradable metals and corrosion.